An experimental study of secondary vortex structure in mixing layers

By J. H. Bell

1. Introduction

This report covers the first eight months of an experimental research project on the secondary vortex structure in plane mixing layers. The aim of the project is to obtain quantitative data on the behavior of the secondary structure in a turbulent mixing layer at reasonable Reynolds numbers ($Re_{\delta_\omega} \sim 50,000$. In particular, we hope to resolve the questions of how the scale of the secondary vortex structure changes with the scale of the mixing layer, and whether the structures are fixed in space, or whether they "meander" in the spanwise direction. Co-investigator for this project is Rabi Mehta, a JIAA research associate.

2. Background

It is well known that the development of plane mixing layers is largely influenced by the formation and interaction of large-scale spanwise vortices (Brown & Roshko 1974). Many of the earlier studies which first determined the important role played by the spanwise vortices also showed the existence of a second organized and persistent vortex structure in the mixing layer. Initial experiments showed that this vortex structure was oriented mostly in the *streamwise* direction, and suggested that its appearance might be related to the appearance of small scales within the flow (Konrad 1977, Breidenthal 1981).

A fairly clear picture of the streamwise vortex structure was produced by subsequent flow visualization experiments (Bernal 1981, Jimenez *et al.* 1985, Lasheras *et al.* 1986, Bernal & Roshko 1986, and Lasheras & Choi 1988), and this is described below. The structure is sketched in figure 1, which is taken from Lasheras *et al.* (1986). It appears that the streamwise vortex structure arises in the braid region of the mixing layer, between the spanwise structures. Residual spanwise vorticity in this region is stretched by the strain field produced by the spanwise structures. The extensional principle axis of the strain field is along a line perpendicular to the spanwise direction and is oriented at an angle to the streamwise direction. The result is the formation of a vortex tube which winds back and forth between adjacent spanwise rollers. When viewed from above, this structure appears to be a row of alternating-sign streamwise vortices embedded in the mixing layer. This picture of the structure has been confirmed by the results of numerical simulations using both the Biot-Savart law (Ashurst & Meiberg, 1988) and the direct Navier-Stokes method (Metcalfe *et al.* 1987).

Despite these results, many features of the streamwise vortex structure are not well understood. This is mostly due to a lack of quantitative information

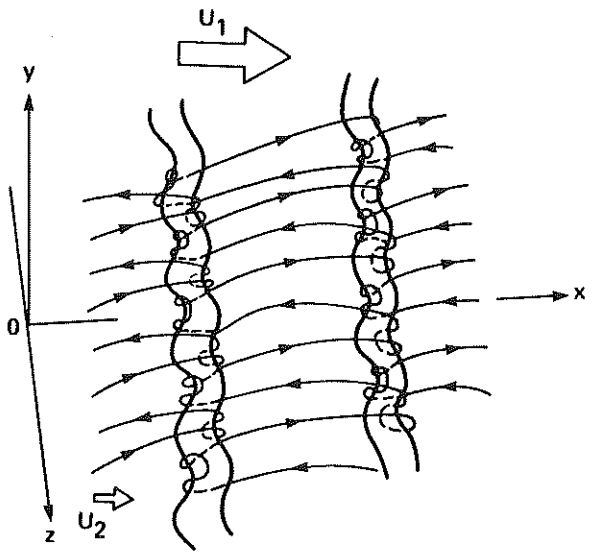

FIGURE 1. Sketch of vortex structure in mixing layers. Thick lines outline the spanwise structures, and the thin lines looping between them represent the streamwise vortex structure. (Taken from Lasheras *et al.* 1986.)

on the development of this structure, which in the past has usually been studied through flow-visualization. Fortunately, the streamwise vortex structure is sufficiently stable that it shows up in the mean flow and can be examined through measurements of mean streamwise vorticity in the mixing layer. This approach was used by the authors in a recent study, which investigated the presence and role of "naturally occurring" streamwise structures in a mixing layer (Bell & Mehta 1989a). A plane, two-stream mixing layer was generated, with a fixed velocity ratio of 0.6 and both initial boundary layers laminar and nominally two-dimensional. Measurements indicated that small spanwise disturbances in the upstream boundary layer on the high speed side of the splitter plate were amplified prior to the roll-up of the spanwise vortex sheet. Actual streamwise vortices were first observed slightly farther downstream, prior to the estimated location of the spanwise vortex roll-up. The streamwise vortices first appeared in widely spaced clusters of 3-4 vortices of both signs, but further downstream, the vortices re-organized to form counter-rotating pairs. The spacing between individual streamwise vortices was found to grow in a stepwise fashion as the mixing layer developed, with the location of the steps corresponding to the estimated locations of pairing of the spanwise vortices. Overall, the streamwise vortex structure scaled approximately with the mixing layer vorticity thickness. The streamwise vortex structures appeared to weaken with streamwise distance, with

the maximum mean vorticity diffusing as approximately $1/X^{1.5}$. The streamwise vorticity was found to be strongly correlated in position, strength, and scale with the secondary shear stress ($\overline{u'w'}$). The $\overline{u'w'}$ data suggested that the streamwise structures persisted through to the self-similar region, although they were very weak by this point and the mixing layer appeared to be nominally two-dimensional.

The present study is an extension of Bell & Mehta (1989a), using more sophisticated instrumentation to examine the role of the streamwise vortex structure in mixing layer development. One particularly interesting question raised by the experimental results relates to the observed decay of the mean streamwise vortex strength with X. This finding is in conflict with the results of direct Navier-Stokes simulations, which show no sign of streamwise vorticity decay (Rogers & Moser 1989). It has been suggested that the discrepancy occurs because the vortices tend to wiggle, or "meander" from side to side in the spanwise direction with increasingly greater amplitude as the flow moves downstream. The increasing amplitude of the meander would presumably reflect the transition of the mixing layer to an increasing turbulent state as the local Reynolds number increased. Once the amplitude of the meander became greater than the spacing between adjacent vortices, the structure would essentially average itself out of the mean flow. However, the streamwise vortex structure should still be detectable by more sophisticated means, such as spatial or temporal correlations. In the present study, it is proposed to apply these techniques to examine the behavior of the secondary vortex structure.

3. Experimental apparatus and techniques

3.1. Pre-existing experimental apparatus

The *Mixing Layer Wind Tunnel* located in the Fluid Mechanics Laboratory at the NASA Ames Research Center was used for all of the work described in this progress report (Fig. 2). The wind tunnel consists of two separate legs which are driven individually by centrifugal blowers connected to variable speed motors. The two blower/motor combinations are sized such that one has three times the flow capacity of the other, although the components downstream of the wide-angle diffusers are identical on the two legs. The two streams are allowed to merge at the sharp edge of the tapered splitter plate. The included angle at the splitter plate edge, which extends 15 cm into the test section, is about 1°, and the edge thickness is approximately 0.25 mm. The test section is 36 cm in the cross-stream direction, 91 cm in the spanwise direction and 366 cm in length. One side-wall is slotted for probe access and flexible for pressure gradient control.

The free-stream velocities within the test section are typically found to remain constant to within 1% of the set value. The measured streamwise turbulence level (u'/U_e) is about 0.15% and the transverse levels (v'/U_e and w'/U_e) are

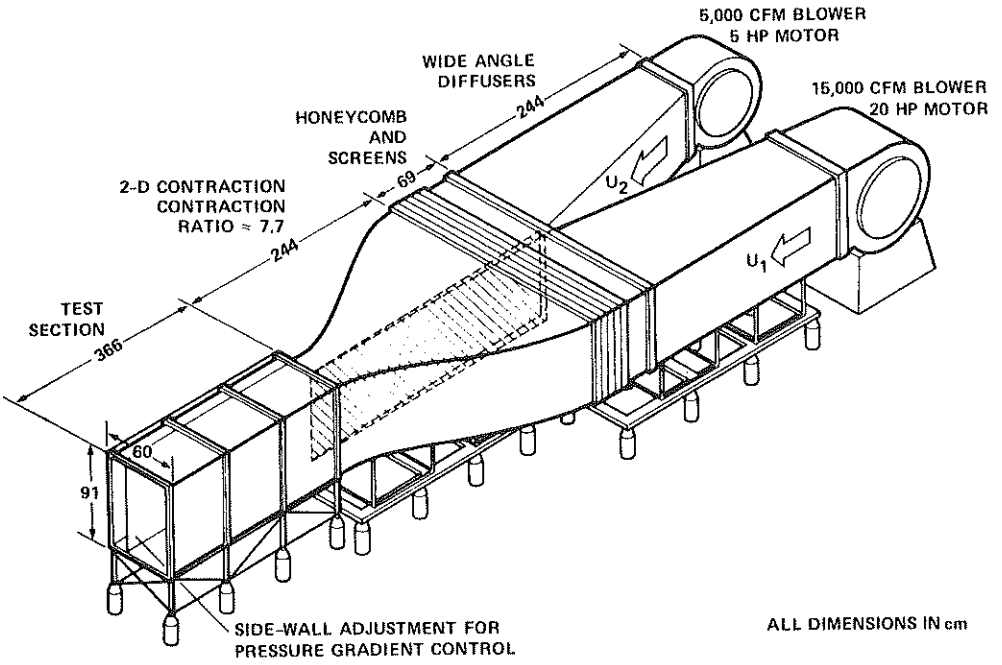

FIGURE 2. Mixing Layer Wind Tunnel.

about 0.05%. The mean core-flow is found to be uniform to within 0.5%, and cross-flow angles are less than 0.25°. Further details of the mixing layer wind tunnel design and calibration are given by Bell & Mehta (1989b).

In the studies described in section 4, measurements were made using a single rotatable cross-wire probe held on a 3-D traverse and linked to a fully automated data acquisition and reduction system controlled by a MicroVax II computer. The cross-wire probe had two 5 μm diameter tungsten sensing elements, each about 1 mm long and positioned about 1 mm apart. The probe was calibrated statically in the potential core of the flow assuming a 'cosine-law' response to yaw, with the effective angle determined by calibration. The analog signals were filtered (low pass at 30 Khz), DC offset, and amplified ($\times$10) before being fed into a NASA-built computer interface. The interface contained a fast sample-and-hold A/D converter with 12 bit resolution and a multiplexer for connection to the computer. Individual statistics were averaged over 5,000 samples obtained at a rate of 400 samples per second.

3.2. New experimental apparatus

As indicated in section 2, single-point, time-averaged measurements are insufficient to fully address the question of how secondary vortex structure develops

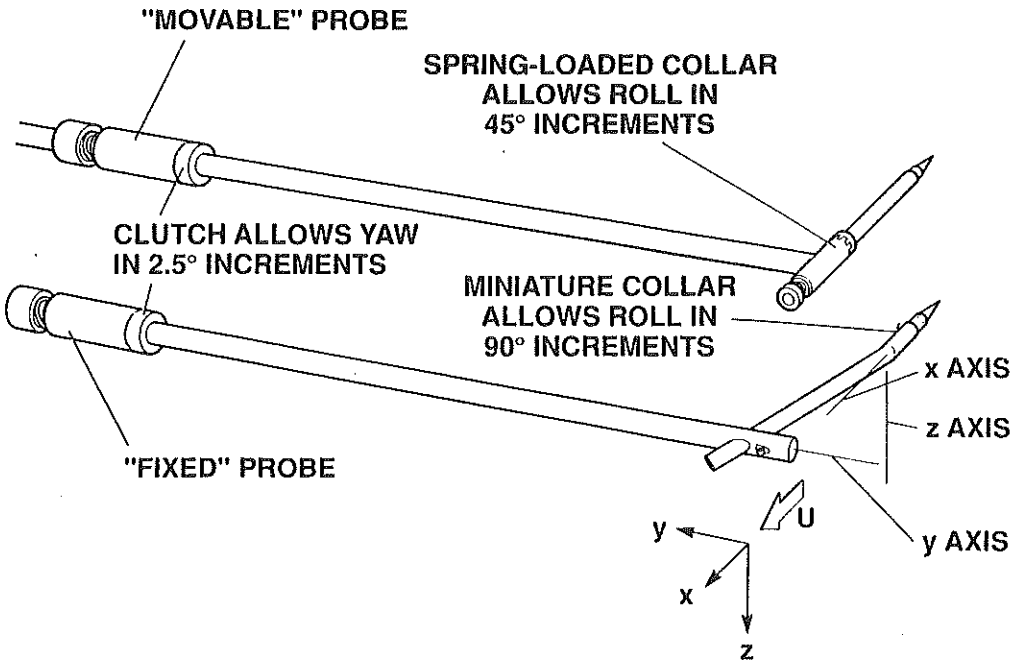

FIGURE 3. Sketch showing new probe holders made for spatial correlation measurements.

in the mixing layer. Accordingly, considerable time has been spent on the construction of new equipment and software for measuring spatial and temporal correlations. The new equipment consists of a pair of new hot-wire probe holders, a second, independent, 2-D traverse system, and a new traverse table. New software has been written to acquire two-point data and compute the correlations, as well as to increase the degree of automation in the data acquisition process.

The two new hot-wire probe holders are sketched in figure 3. Both probe holders allow the crossed hot-wire probes to be yawed at 2.5° intervals for precise angle calibrations. The larger "movable" probe can be rolled at 45° intervals, allowing measurements of all six independent components of the Reynolds stress tensor, as well as the three components of mean velocity. The smaller "fixed" probe can be rolled at 90° intervals. Both probe holders will be capable of moving independently on separate traversing systems. In practice, however, the "fixed" probe holder will be left at one point in the flow, while the "movable" probe holder is traversed automatically around it, to obtain correlation measurements. The movable probe holder is designed primarily for ease of use, and is mounted on the original computer-controlled 3-D traverse system. The fixed probe holder is designed with an angled head, so that the two hot-wire probes can be brought as close together as possible. The minimum probe separation is 6 mm, which, in the region under investigation, is approximately 1/10th the mixing layer thickness,

and 1/5th the radius of the streamwise vortices. The fixed probe is mounted on a 2-D traverse system, which rests within the 3-D traverse for the movable probe.

A new table for the combined probe traversing mechanism has been constructed. The old traverse table, made from wood, had to be laboriously shifted and re-leveled at each new measurement station. Careful leveling is necessary because the angle the probe makes with the flow must be carefully maintained from one station to the next in order to make consistent measurements of the secondary velocities, which are comparatively small. The new traverse table is more stable than the old one, and has a more effective leveling system. This allows the probes to be shifted between measurement stations much more quickly and accurately, increasing both the overall rate at which data is acquired and its repeatability.

Under the old system, velocity data from the crossed hot-wire was reduced on-line. Raw data was not stored. The greater volume of data produced by the dual probes makes real-time data reduction impractical, while the recent acquisition by the Fluid Mechanics Lab of an Exabyte EXB-8200 8mm helical scan tape drive makes it considerably easier to store large quantities of raw data. As a result, new software has been written to allow the raw data to be stored and transferred to tape with extensive off-line data reduction. The stored raw data will form a database from which any temporal or spatial correlation implicit in the original measurements can be retrieved. Another major aim of the software upgrade has been to further automate the data acquisition procedure. The new probe holder design allows the crossed hot-wire calibration procedure to be partially automated. As a result, the calibrations can be automatically checked at periodic intervals during a run. This will result in longer running times, a lower level of operator intervention, and lower errors due to hot-wire drift.

3.3. New measurement techniques: application to the problem

A simple relationship between spatial correlation data and the actual coherent structures in a turbulent flow can rarely be established. Considerable care must be exercised in postulating the form of a turbulent structure from the correlation data, and in fact some controversy has arisen in the past concerning the interpretation of correlation measurements in mixing layers (Chandrsuda *et al.* 1978, Wygnanski *et al.* 1979, Wood 1980). In the present case, the task is considerably easier. The general shape of the coherent structures has already been discovered through flow visualization, and it is only necessary to determine their scale and strength. Thus, it is reasonable to search for the particular correlation which is most likely to give unambiguous data concerning the behavior of the structures.

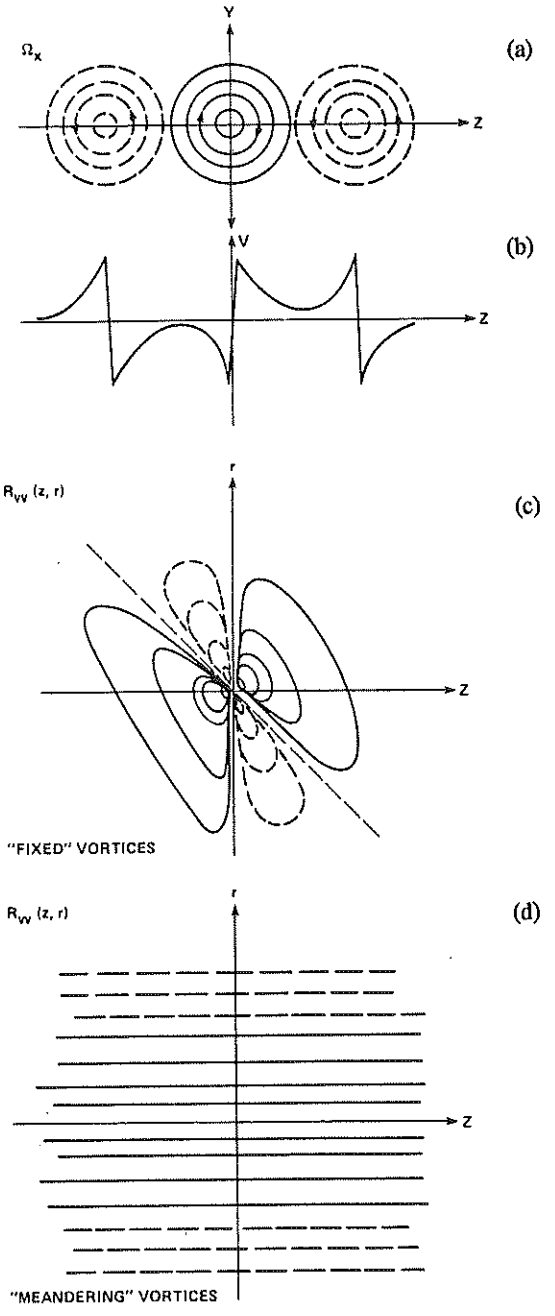

FIGURE 4. Sketches showing details of proposed spatial correlation measurements. z is the spanwise location of the fixed probe, r is the spanwise separation between probes. a) Sketch of streamwise vorticity field in mixing layer. b) Level of cross-stream velocity along a line through the centers of the vortices. c) Sketch of spatial correlation R_{vv} for the case of fixed streamwise vortices. d) Sketch of spatial correlation R_{vv} for the case of meandering streamwise vortices.

To address the question of spanwise meander of the streamwise vortex structures, the best quantity to examine appears to be the variation of the cross-stream velocity correlation in the spanwise direction, i.e., $R_{vv}(0,0,r)$. Imagine that the shear layer contains a row of alternating-sign streamwise vortices, as diagrammed in figure 4a. A distinctive pattern of cross-stream velocity is produced. This is demonstrated in figure 4b, which shows the variation of V with Z along a line drawn through the vortex centers. The cross-stream velocity rapidly changes sign across the core of a streamwise vortex. If correlation measurements are made along a line passing through the streamwise vortex cores in the spanwise direction, there will be a zero-crossing at a separation corresponding to the radius of the vortices. This correlation will be observed even if spanwise meander has reduced the *mean* streamwise vorticity to zero. The amplitude of the meander can also be determined from the variation of R_{vv} with both the spanwise location of the fixed probe (z) and the spanwise separation of the probes (r). If the streamwise vortex structure is fixed in the spanwise direction, the variation of R_{vv} with z and r can be easily calculated from the V vs z curve shown in figure 4b. The resulting contour plot is shown in figure 4c. If the structure meanders over a distance larger than the radius of the streamwise vortices, the very different correlation shown in figure 4d will be obtained. In this case, while there is no dependence on the location of the fixed probe (i.e. z) and no detectable mean vorticity, the variation with probe separation r suffices to establish the presence and radius of the streamwise structures.

4. Effect of initial conditions on mixing layer structure

As an interim study while the new instrumentation was designed and built, it was decided to examine the effects of initial conditions on streamwise vorticity in mixing layers. The results of Bell & Mehta (1989a), for a mixing layer originating from a splitter plate with laminar initial boundary layers, were used as a base case for comparison. Hereinafter, this case is referred to as the *undisturbed* case. The second case was that of a mixing layer originating from turbulent initial boundary layers, but with the same operating conditions as Bell & Mehta (1989a). This case is referred to as the *tripped* case. No mean streamwise vorticity was found in the tripped mixing layer, and a difference between the far-field growth rates of the tripped and undisturbed cases was noted. It was speculated that the difference in growth rates, which has been observed by previous researchers (Browand & Latigo 1979, and Mehta & Westphal 1986) was related to the absence of mean streamwise vorticity in the tripped case. Accordingly, a third or *vortex generator* case was studied, in which streamwise vorticity was injected into the tripped mixing layer by means of a row of vortex generators mounted on one side of the splitter plate.

4.1. Experimental setup

In all three cases, the free-stream velocities were set at 15 m/s on the high-speed side and 9 m/s on the low-speed side, thus giving a mixing layer with velocity ratio $U_2/U_1 = 0.6$. In the tripped case, the boundary layers on the splitter plate were perturbed using round wire trips about 0.75 mm diameter on the high-speed side and 1.2 mm diameter on the low-speed side. The wire trips were installed 15 cm upstream of the trailing edge to allow the boundary layers to recover from the perturbation. Well-developed turbulent boundary layers were produced on both sides of the splitter plate; details of the boundary layers for the first two cases are summarized below in Table 1.

Table 1. Initial Boundary Layer Properties

Condition	U_e (m/s)	δ_{99} (cm)	θ (cm)	Re_θ	H	C_f $\times 10^3$
High-Speed Side, Undisturbed	15.0	0.398	0.0526	525	2.52	0.87
Low-Speed Side, Undisturbed	9.0	0.441	0.0606	362	2.24	1.56
High-Speed Side, Tripped	15.0	0.758	0.0820	804	1.49	5.30
Low-Speed Side, Tripped	9.0	0.851	0.0941	567	1.50	4.86

In the vortex generator case, streamwise vortices were injected into the mixing layer by a row of half-delta wing vortex generators placed on the high-speed side of the splitter plate, 2.54 cm ahead of the trailing edge. Both initial boundary layers had been tripped with round wires as described in the second case. The vortex generators were installed at alternating positive and negative angles of attack with their trailing edges spaced 1.91 cm apart, so as to produce an evenly-spaced row of counter-rotating streamwise vortices. Each vortex generator had a 6.4 mm semi-span, a 68° sweep angle, and was placed at an angle of attack of $\pm 17°$. The vortex generator spacing was chosen to be comparable to the Kelvin-Helmholtz wavelength, and the semi-span was chosen to be approximately equal to the local boundary layer thickness.

Data were obtained in the uv- and uw-planes with a cross-wire probe at nine streamwise stations for the undisturbed case and at eight stations each for the two other cases. In each case, measurements were made at corresponding positions within the test section, located between X $\sim$ 10 to 250 cm downstream of the splitter plate. In the undisturbed case, the last station is $4760\theta_1$ downstream of the splitter plate trailing edge, where θ_1 is the momentum thickness of the high-speed side splitter plate boundary layer. In the two cases with turbulent initial boundary layers, the last station is $3050\theta_1$ downstream of the trailing edge. At each station, data were obtained in a cross-sectional plane which typically extended over 20 points in the cross-stream direction and 60 points in

the spanwise direction. The spanwise extent of the data set ranged from three to ten mixing layer thicknesses, depending on the streamwise location. All the global properties presented below were *spanwise-averaged* for all cases. The measurements of U, W and $\overline{u'w'}$ were corrected for mean streamwise velocity gradient ($\partial U/\partial Y$) effects, assuming a linear variation in U between the cross-wire sensors (Bell & Mehta 1989a). The streamwise component of mean vorticity ($\omega_x = \partial W/\partial Y - \partial V/\partial Z$) was computed using the central difference method. The overall circulation was defined as the surface integral of the streamwise vorticity over the cross-flow plane with vorticity levels less than 10% of the maximum value being set to zero in order to provide immunity from "noise".

4.2. Results and discussion

Contour plots of mixing layer properties at a representative station show clear differences in the three cases. Figures 5-7 show selected properties measured at $X = 57.3$ cm, which is just downstream of the estimated location of the second vortex pairing. The mean streamwise vorticity contours show the most marked difference between the three cases. In the undisturbed case (figure 5a), an irregular row of $8 - 10$ streamwise vortices of varying strengths can be easily made out. In contrast, the tripped case (figure 5b) has a much lower level of vorticity in an irregular pattern, not at all suggestive of concentrated streamwise vortices. In the vortex generator case, a single row of 11 round, well-defined counter-rotating vortices are clearly observed, with the magnitudes of the peak levels approximately the same. The spacing between the vortices is 2 cm, approximately the same as the spacing between the vortex generator trailing edges. In the undisturbed and vortex generator cases, the mean streamwise vorticity is strongest at the first measurement station ($X = 7.8$ cm), and its effects on the other flow quantities are greatest at this location.

The presence of mean streamwise vorticity leads to spanwise variation of the mixing layer properties. Contours of mean streamwise velocity are shown for the three cases in figure 6. In the undisturbed case (figure 6a), there is an irregular distortion of the mean flow, corresponding to the presence of the streamwise vortices. The tripped case (figure 6b) displays very little spanwise variation — the flow appears essentially two-dimensional. The contours for the vortex generator case (figure 6c) give an idea of the strength of the injected vortices. A very regular, well-defined spanwise wavelength can be observed in the contours, the "peaks" and "valleys" of which mark regions of common flow up or down, in between the vortices. Similar behavior is seen in the turbulence quantities, as shown in figure 7, which plots contours of twice the turbulent kinetic energy ($\overline{q^2}$). The undisturbed case (figure 7a) displays an irregular variation associated with the streamwise vortices while the tripped case (figure 7b) turbulence distribution is essentially two-dimensional. In the vortex generator case (figure 7c), the pattern is quite well-marked and similar to that of the mean velocity, with the presence of local peaks of $\overline{q^2}$ near the centerline.

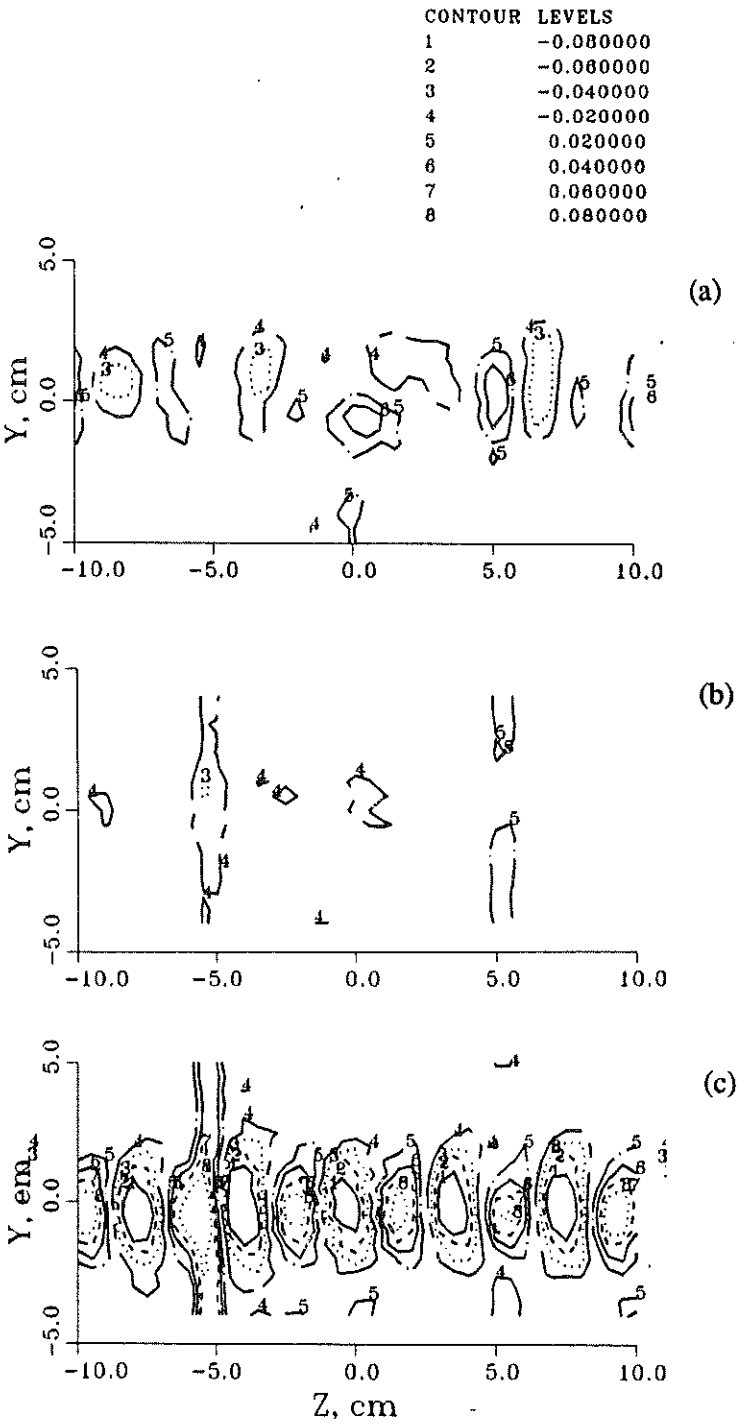

FIGURE 5. Contours of mean streamwise vorticity Ω_x/U_0 (cm^{-1}) at $X = 57.3$ cm. a) Undisturbed case, b) Tripped case, c) Vortex generator case.

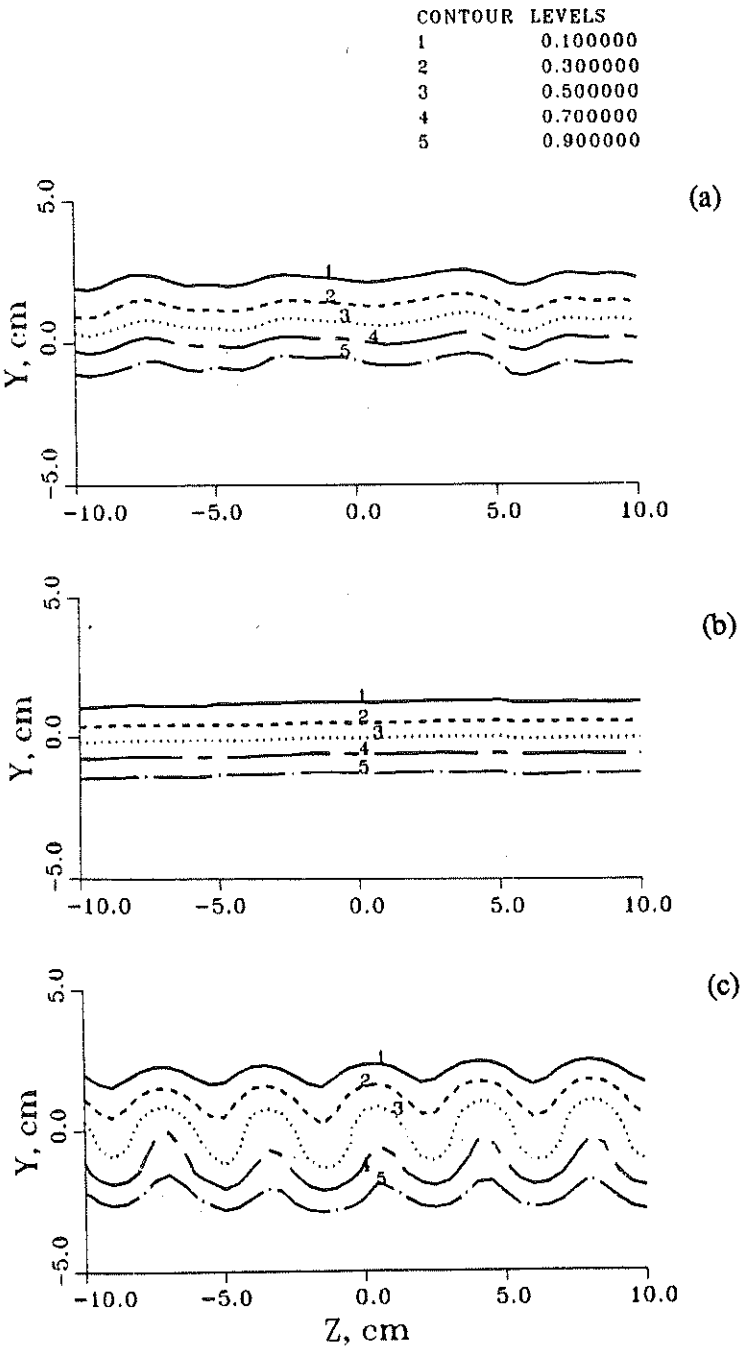

FIGURE 6. Contours of mean streamwise velocity U/U_0 at $X = 57.3$ cm. a) Undisturbed case, b) Tripped case, c) Vortex generator case.

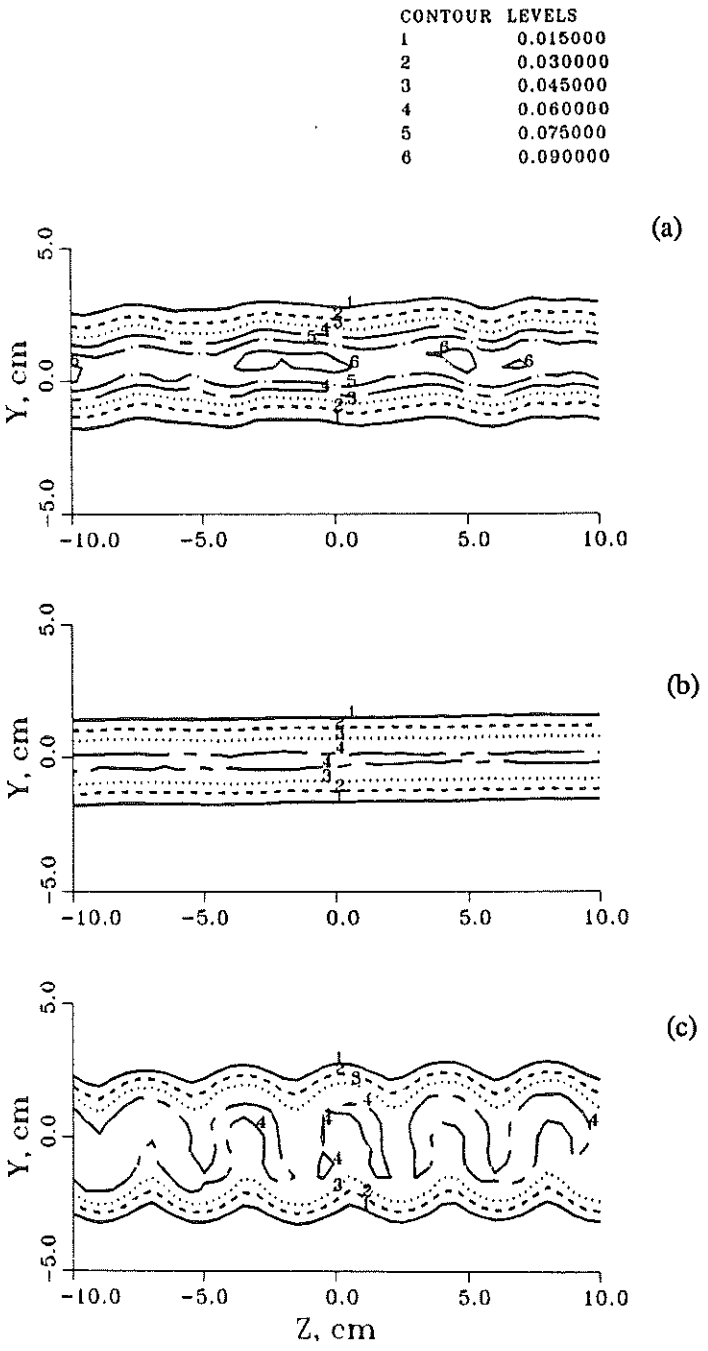

FIGURE 7. Contours of turbulent kinetic energy $\overline{q^2}/{U_0}^2$ at $X = 57.3$ cm. a) Undisturbed case, b) Tripped case, c) Vortex generator case.

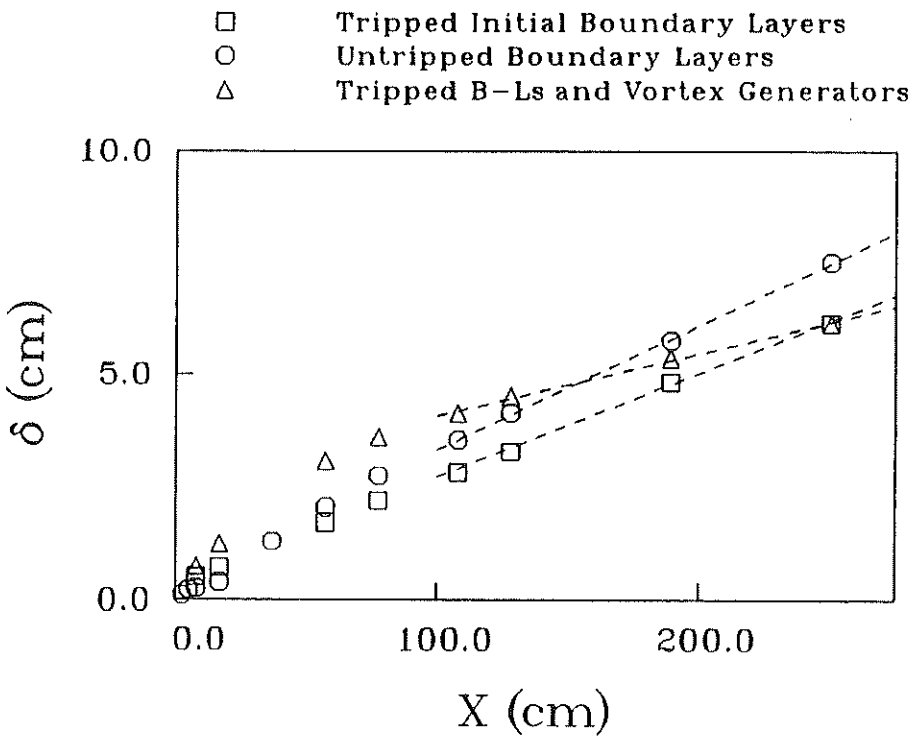

FIGURE 8. Mixing layer thickness (determined as described in text), versus streamwise distance.

The differences between the three cases shown in the contour plots reflect a difference in the global mixing layer properties. Figure 8 shows the mixing layer thickness δ, determined by fitting the mean velocity profile to an error function, for all three cases. (Mixing layer thickness has been determined by fitting the normalized mean velocity data to an error function profile shape: $U/(U_1-U_2) = [1+erf(\zeta)]/2$, where ζ is the normalized cross-stream coordinate: $\zeta = (y-y_0)/\delta$. The values of δ and y_0 are taken to be the mixing layer thickness and centerline location, respectively.) The three cases have very different growth rates, especially in the far-field, where linear growth is expected. The tripped case growth rate in the linear region is $d\delta/dx = 0.023$, quite close to the accepted value for a mixing layer with this velocity ratio. But the far-field growth rate for the undisturbed case is 20% higher than that for the tripped case. As noted above, similar differences in growth rate have been reported previously in the literature. Spanwise averaging of the mixing layer properties, employed for the first time in this study, shows that the difference in growth rates persists across the mixing layer span.

Since the undisturbed case contains significant mean streamwise vorticity while the tripped case does not, it was expected that the injection of streamwise

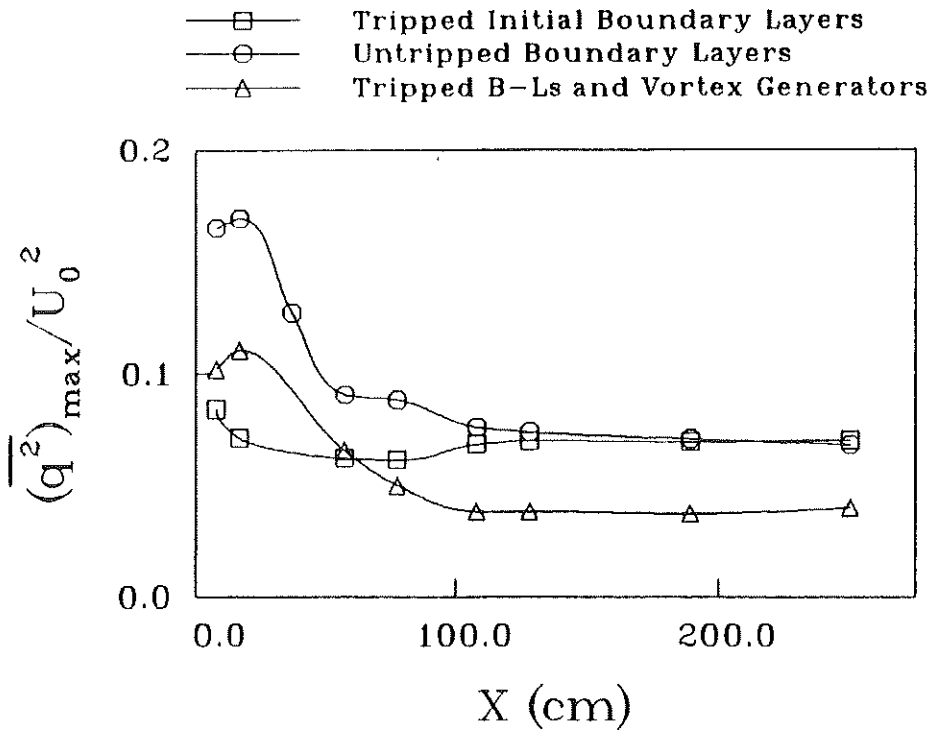

FIGURE 9. Maximum turbulent kinetic energy versus streamwise distance.

vorticity would increase the growth rate. But, although the growth is high initially in this case (for $X \leq 60$ cm), the far-field growth rate is extremely low — only 61% of the tripped case growth rate. Since the mixing layer growth rate is so drastically affected by the vorticity injection, the Reynolds stresses would be expected to show a comparable effect. This is indeed the case as seen in the streamwise development of the peak turbulent kinetic energy, $\overline{q^2}_{max}$ (figure 9). The tripped and undisturbed cases asymptote to about the same constant level beyond $X \sim 125$ cm. The vortex generator case also achieves a constant level by that streamwise location, but the asymptotic level is significantly lower. This is not too surprising given the lower cross-stream velocity gradients in this case. At the last station, a very slight upturn in the $\overline{q^2}_{max}$ level for the vortex generator case is noticeable. Measurements at a station some 30 cm farther downstream (not shown) also show a slightly higher turbulence level, but their accuracy is suspect due to test section end effects. This behavior *may* indicate that at some distance farther downstream, this case will recover to a higher level of Reynolds stresses, and presumably a higher growth rate as well.

The behavior of the injected streamwise vorticity in vortex generator case is compared to that of the "naturally occurring" vorticity, measured in the undisturbed case, in figure 10. The peak vorticity and circulation data presented in

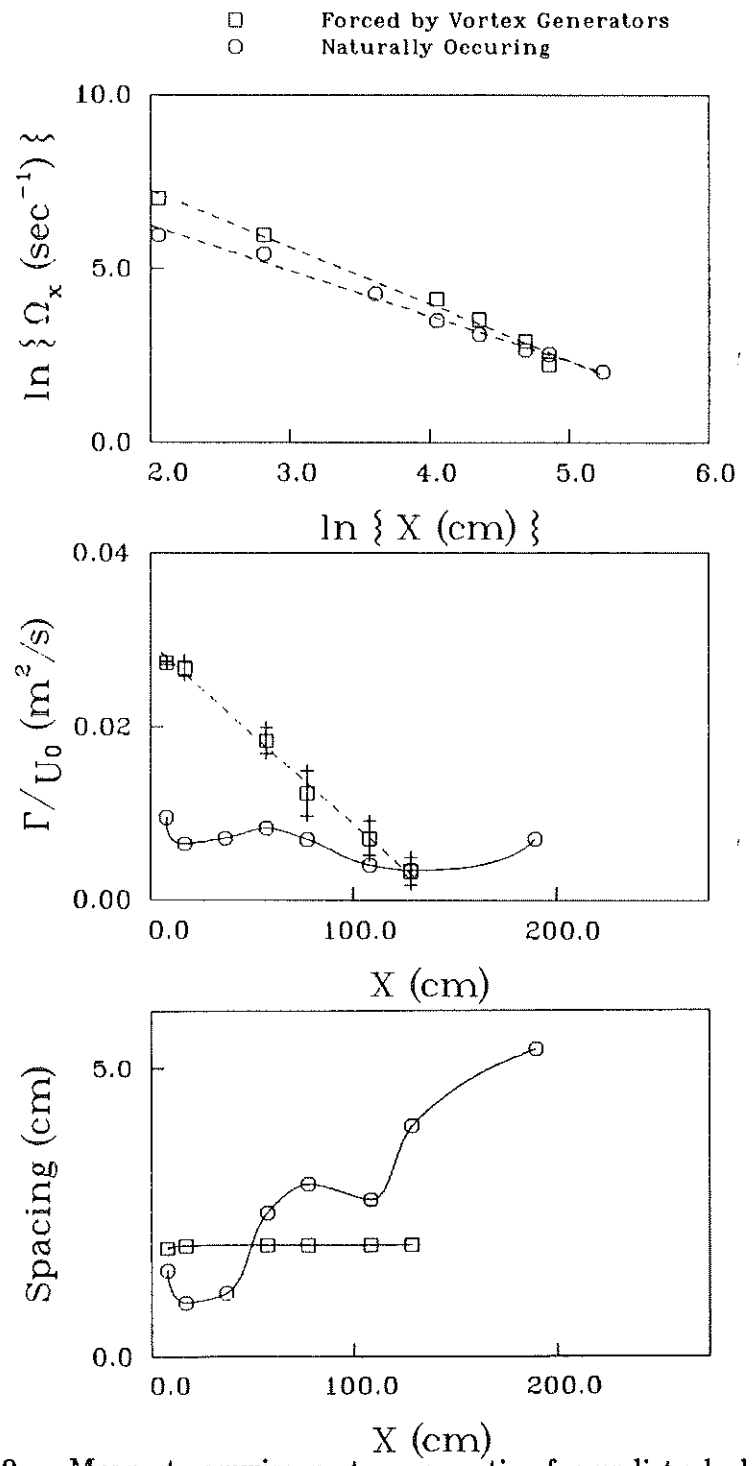

FIGURE 10. Mean streamwise vortex properties for undisturbed and vortex generator cases. a) Peak streamwise vorticity vs X, log-log scale, b) Streamwise vortex circulation vs X, c) Streamwise vortex spacing vs X.

figure 10 are left unnormalized. The most appropriate normalizing parameters — the initial strength and circulation of the spanwise structures — can only be estimated in the present study. Mean spanwise vorticity, $\Omega_z = (\frac{\partial V}{\partial x} - \frac{\partial U}{\partial y})$ was estimated by assuming the $\frac{\partial V}{\partial y}$ term is negligible. Spanwise vortex circulation was estimated using an initial streamwise wavelength determined by the convection velocity and the measured natural frequency of the mixing layer. (For the undisturbed case, the estimated values at about the location of the first roll-up are: $\Omega_{z_{max}} = 1400$ s$_1$ and $\Gamma_z = 0.11$ m^2/s. For the vortex generator case, the estimate is made more uncertain by the highly distorted state of the mixing layer and the lack of a clearly observable natural frequency. In this case, the estimated values are: $\Omega_{z_{max}} = 1100$ s$_1$ and $\Gamma_z = 0.11$ m^2/s.)

The streamwise development of the peak mean vorticity for two cases is presented on a log-log scale in Fig. 10a. The decay is roughly linear on this scale, indicating a power-law decay rate. Although the peak initial levels for the injected vorticity are considerably higher, the decay rate is also faster; the naturally occurring vorticity was found to decay as $1/X^{1.5}$, whereas the injected vorticity decays as $1/X^{1.8}$. Beyond the station at $X \sim 100$ cm, the peak levels for the two cases are seen to be comparable. As discussed previously, this apparent reduction in vortex strength may actually be due to the increasingly large meander of vortices of constant strength; spatial correlation measurements will be conducted in the future to establish whether or not this is the case. The vortex circulation (Fig. 10b) shows very different behavior for the two cases. The naturally occurring vortex circulation shows a very slow decrease, with a small intermediate peak at $X \sim 60$ cm — this was associated with the change in scale of the streamwise vortex structure (described below). However, the injected vortex circulation shows a relatively fast linear decay and by $X \sim 125$ cm, the level is comparable to that of the naturally occurring vortices. The mean spacing of the streamwise vortices can be easily found by counting the number of vortices present at each station. The vortex spacing in the undisturbed case increases in a step-wise fashion, scaling approximately as the mixing layer vorticity thickness (Fig. 10c). On the other hand, the spacing for the injected vortices is *constant* within the measurement domain. This may simply be due to the fact that the injected vortices are of equal strength and spacing, unlike the naturally occurring structures, and so there is no tendency for self-induced motion. Another possibility, related to the pairing of the *spanwise* structures, is discussed below.

4.3. Conclusions

The original purpose of injecting the streamwise vorticity into the tripped mixing layer was to try and increase its growth rate to a level more comparable to that of the undisturbed layer. The initial ($X \leq 60$ cm) growth rate is indeed increased significantly due to the extra entrainment provided by the streamwise structures. However, the growth rate further downstream ($X \geq 100$ cm) is

reduced drastically over both the tripped and untripped cases. A possible explanation for this change can be made by postulating that the streamwise vortex structure affects the pairing of the spanwise vortices. Most of the growth of a mixing layer occurs due to entrainment during the pairing process of the nominally two-dimensional spanwise vortical structures (Sandham *et al.* 1988). If the spanwise structures were altered so as to reduce the pairing rate, entrainment by the mixing layer, and thus its growth rate, would be decreased.

The naturally occurring streamwise vorticity in the undisturbed case first appears in the regions of maximum extensional strain, in the braid region. The two structures become interlaced in such a way that, in flow-visualizations, it appears that the only effect of the streamwise structure on the spanwise is to produce a regular, gentle undulation in the latter (Lasheras *et al.* 1986). Therefore, the entrainment due to the spanwise structures proceeds undisturbed; total growth may in fact be enhanced by the additional entrainment in the braids due to the streamwise structures. However, the injected vorticity in the vortex generator case imposes its own pattern on the spanwise structures, as indicated by the gross distortions in the mean velocity contours. It is possible that this changes the pairing process, reducing the pairing rate. In the near-field, entrainment by the streamwise structures more than makes up for this deficit. However, entrainment due to the streamwise vortices decreases much faster than the spanwise structures recover, so at some point the overall entrainment rate is reduced, and hence the growth rate of the mixing layer drops. This hypothesis is also consistent with differences noted in the behavior of the streamwise vortices in the two cases. Previous investigations have suggested that the scale change in the streamwise vortices occurs during the pairing of the spanwise rollers (Jimenez *et al.* 1985, Bell & Mehta 1989a). The fact that a scale change is not observed in the vortex generator case suggests that the pairing of the spanwise rollers has been suppressed.

The mixing layer with vorticity injection maintains a lower growth rate and turbulence levels out to the end of the measurement region in the current study. Although there is some evidence of an upward trend at the last measurement station, the data is not sufficiently extensive to determine when, if ever, the vortex generator case will recover to a higher turbulence level and growth rates. The absence of such a recovery would, of course, indicate that more than one asymptotic structure is possible in mixing layers.

5. Future plans

The equipment and software for spatial correlation measurements is currently in the final test phase. Once the checkout is complete, work will commence on:

- A study of the variation of $R_{vv}(0,0,r)$ in the undisturbed mixing layer. An examination of this quantity will show the extent of spanwise meander of the streamwise vortex structure.

- A similar study of the tripped mixing layer. In this case, the mean streamwise vortex structure is entirely absent. Correlation measurements will determine if it is actually present, but masked by a high level of meander.
- A study of the vortex generator case, which will attempt to determine what sort of turbulence structure is responsible for the lower growth rate. Correlation measurements should be able to determine the extent to which the streamwise vortex structure influences the development of the spanwise rollers.

In addition to these studies, which are designed to take advantage of the new instrumentation, two additional cases are being considered:

- A repeat of the vortex generator case, at twice the original free-stream velocities, but with the same velocity ratio. This would approximately double the nondimensionalized development distance, as determined by either Reynolds number or initial mixing layer thickness. Thus, it should be possible to determine when, if ever, the effect of initial conditions relaxes, and a more "normal" growth rate is recovered. Requiring no complex measurements, this study can be accomplished fairly quickly.
- A study of a mixing layer originating from a splitter plate with a corrugated end. Such a splitter plate would inject cross-stream vorticity into the mixing layer, in a manner analogous to the way that the vortex generator case injects streamwise vorticity. Thus, this study would form a natural complement to the vortex generator case. Although this flow has been previously studied at low Reynolds numbers through flow-visualization (Lasheras & Choi, 1988), the unusual behavior of the vortex-generator case suggests that it merits a second, more intensive look.

Acknowledgments

I would like to thank my co-investigator, Dr. Rabindra D. Mehta. Although not associated with the C.T.R., Dr. Mehta has participated wholeheartedly in this project, and it owes much to his expertise and assistance, for which I am very grateful. Dr. Mehta was supported by NASA Grant NCC-2-55 from the Fluid Dynamics Research Branch, NASA Ames Research Center.

REFERENCES

ASHURST, W. T., & MEIBURG, E. 1988 Three-Dimensional Shear Layers via Vortex Dynamics.. *J. Fluid Mech.* **189**, 87-116.

BELL, J. H. & MEHTA, R. D. 1989a Three-Dimensional Structure of a Plane Mixing Layer. AIAA Paper 89-0124. Also, JIAA Report TR-90, Dept. of Aero/Astro, Stanford University.

BELL, J. H. & MEHTA, R. D. 1989b Design and Calibration of the Mixing Layer Wind Tunnel. JIAA Report TR-89, Dept. of Aero/Astro, Stanford University.

BERNAL, L. P. 1981 The Coherent Structure of Turbulent Mixing Layers. Ph.D. Thesis, California Institute of Technology.

BERNAL, L. P. & ROSHKO, A. 1986 Streamwise Vortex Structure in Plane Mixing Layers. *J. Fluid Mech.* **170**, 499-525.

BREIDENTHAL, R. 1981 Structure in Turbulent Mixing Layers and Wakes using a Chemical Reaction. *J. Fluid Mech.*, **109**, 1-24.

BROWAND, F. K. & LATIGO, B. O. 1979 Growth of the Two-Dimensional Mixing Layer from a Turbulent and Nonturbulent Boundary Layer. *Phy. Fluids*, **22**, pp. 1011-1019.

BROWN, G. L. & ROSHKO, A. 1974 On Density Effects and Large Structure in Turbulent Mixing Layers. *J. Fluid Mech.*, **64**, pp. 775-816.

CHANDRSUDA, C., MEHTA, R. D., WEIR, A. D., & BRADSHAW, P. 1978 Effect of Free-stream Turbulence on Large Structures in Turbulent Mixing Layers. *J. Fluid Mech.*, **85**, pp. 693-704.

JIMENEZ, J., COGOLLOS, M., & BERNAL, L. P. 1985 A Perspective View of the Plane Mixing Layer, *J. Fluid Mech.*, **152**, pp. 125-143.

KONRAD, J. H. 1977 An Experimental Investigation of Mixing in Two-Dimensional Turbulent Shear Flows with Applications to Diffusion-Limited Chemical Reactions, Ph.D. Thesis, California Institute of Technology, and Project SQUID Technical Report CIT-8-PU, Dec. 1976.

LASHERAS, J. C., CHO, J. S. & MAXWORTHY, T. 1986 On the Origin and Evolution of Streamwise Vortical Structures in a Plane, Free Shear Layer. *J. Fluid Mech.*, **172**, pp. 231-258.

LASHERAS, J. C. & CHOI, H. 1988 Stability of a Plane Turbulent Shear Layer to Axial Perturbations. *J. Fluid Mech.*, **189**, pp. 53-86.

MEHTA, R. D. & WESTPHAL, R. V. 1986 Near-Field Turbulence Properties of Single- and Two-Stream Plane Mixing Layers. *Exp. in Fluids*, 4, pp. 257-266.

METCALFE, R. W., ORSZAG, S. A., BRACHET, M. E., MENON, S., & RILEY, J. J. 1987 Secondary Instability of a Temporally Growing Mixing Layer. *J. Fluid Mech.*, **184**, pp. 207-243.

ROGERS, M. M., & MOSER, R. D. 1989 The Development of Three-Dimensional Temporally-evolving Mixing Layers. Proceedings of the 7th Symposium on Turbulent Shear Flows, Aug. 21-23, Stanford University, *vol.* 1, pp 9.3.1-9.3.6.

SANDHAM, N. D., MUNGAL, M. G., BROADWELL, J. E., & REYNOLDS, W. C. 1988 Scalar Entrainment in Mixing Layers. Proceedings of the 1988 Summer Program, Center for Turbulence Research, CTR-S88, Dec. 1988, pp. 69-76.

WOOD, D. H. 1980 A Reattaching, Turbulent, Thin Shear Layer, Ph.D. Thesis, Dept. of Aeronautics, Imperial College, University of London.

WYGNANSKI, I., OSTER, D., FIEDLER, H., & DZIOMBA, B. 1979 On the Perseverance of a Quasi-Two-Dimensional Eddy-Structure in a Turbulent Mixing Layer. *J. Fluid Mech.*, **93**, pp. 325-335.